

1 **Improving estimates of ecosystem metabolism computed from**
2 **dissolved oxygen time series**

3 **Marcus W. Beck¹, Michael C. Murrell², James D. Hagy III²**

¹ORISE Research Participation Program

*USEPA National Health and Environmental Effects Research Laboratory
Gulf Ecology Division, 1 Sabine Island Drive, Gulf Breeze, FL 32561
Phone: 850-934-2480, Fax: 850-934-2401, Email: beck.marcus@epa.gov*

*²USEPA National Health and Environmental Effects Research Laboratory
Gulf Ecology Division, 1 Sabine Island Drive, Gulf Breeze, FL 32561*

Phone: 850-934-2433, Fax: 850-934-2401, Email: murrell.michael@epa.gov

*³USEPA National Health and Environmental Effects Research Laboratory
Gulf Ecology Division, 1 Sabine Island Drive, Gulf Breeze, FL 32561*

Phone: 850-934-2455, Fax: 850-934-2401, Email: hagy.jim@epa.gov

Running head: Improving Estimates of Estuary Metabolism

4 *Acknowledgments*

5 We acknowledge the significant efforts of research staff and field crews from the System
6 Wide Monitoring Program of the National Estuarine Research Reserve System for providing
7 access to high quality data sets. We thank Dr. Jane Caffrey for stimulating discussion and
8 previous work on applications of the open-water method to estuarine monitoring data. This study
9 was funded by the US Environmental Protection Agency, but the contents are solely the views of
10 the authors. Use of trade names does not constitute endorsement by the US government.

Abstract

In aquatic ecosystems, time series of dissolved oxygen (DO) have been used to compute estimates of integrated ecosystem metabolism. Central to this open water or “Odum” method is the assumption that the dissolved oxygen time series is a Lagrangian specification of the flow field. However, most DO time series are collected at fixed locations, such the method must assume that changes in dissolved oxygen principally reflect ecosystem metabolism and that effects due to advection or mixing can be neglected. A statistical model using weighted regression was applied to separate variability in DO associated with metabolism from tidal variation or other advection in estuaries, thereby helping to partially relax this assumption and improve estimates of ecosystem metabolism. The method was developed and tested using a simulated DO time series with known biological and physical components, and then applied to one year of continuous monitoring data from four water quality stations within the National Estuarine Research Reserve System. Overall, the approach is a useful way to reduce variability in estimates of ecosystem metabolism caused by advection, particularly when the magnitude of tidal influence is high. By reducing the effects of physical transport on metabolism estimates, there may be increased potential to empirically relate metabolic rates to causal factors on times scales of several days to several weeks. Estimates of variability associated with physical advection may also be more interpretable, since convolution of physical and biological effects can be reduced, providing increased potential to resolve differences in metabolism across a mosaic of estuarine habitats.

Introduction

{intro}

Time series of dissolved oxygen are increasingly used to estimate ecosystem metabolism (Kemp and Testa 2012, Needoba et al. 2012). Integrated measures of metabolism describe the balance between production and respiration processes that create and consume organic matter, respectively. Although metabolic rates vary naturally at different spatial and temporal scales (Ziegler and Benner 1998, Caffrey 2004, Russell and Montagna 2007), anthropogenic nutrient sources are often contributing factors that increase rates of production (Nixon 1995, NRC 2000). Inputs of limiting nutrients beyond background concentrations may decrease the resilience of an ecosystem such that higher rates of production are coupled with higher biological oxygen demand (Yin et al. 2004, Kemp et al. 2009). Cultural eutrophication is frequently linked to declines in water quality through lower levels of dissolved oxygen, degradation in aquatic vegetation habitat, and increased frequency of harmful algal blooms (Cloern 1996, Short and Wyllie-Echeverria 1996, Rabalais et al. 2002, Diaz and Rosenberg 2008). Reliable estimates of ecosystem metabolism are critical for measuring both background rates of production and potential impacts of human activities on ecosystem condition.

Open-water techniques have been used for decades to infer metabolic rates using *in situ* measurements from continuous monitoring data (Odum 1956). Daily integrated measurements of metabolism represent the balance between daytime production and nighttime respiration. The open-water method uses the diel fluctuation of dissolved oxygen to estimate ecosystem metabolism, after correcting for air-water gas exchange (Kemp and Testa 2012). As with any method, the ability to accurately estimate whole system metabolism depends on the degree to which assumptions of the theory are met. The fundamental assumption is that the time series of

{acro:DO}

dissolved oxygen (DO) represents a Lagrangian specification of the flow field that describes the same water mass over time (Needoba et al. 2012). The Lagrangian specification assumes that the time series characterizes individual fluid parcels regardless of location, as in a parcel of water moving with the tide. In reality, most DO time series are collected at fixed locations such as a mooring or dock, which is characterized by an Eulerian specification of the flow field. Time series at fixed locations may characterize water masses with different metabolic histories if water particles are transported by physical advection. A Lagrangian flow field is often assumed, such that estimates of metabolism may be inaccurate if substantial variation in water column mixing occurs throughout the period of observation (Kemp and Boynton 1980, Russell and Montagna 2007). Given this critical challenge, the open-water method has been used with varying success in lakes (Staehr et al. 2010, Coloso et al. 2011, Batt and Carpenter 2012) and estuaries (Caffrey 2004, Russell and Montagna 2007, Caffrey et al. 2013). Appropriate placement of monitoring sondes, sampling frequency and duration, and reliability of data from single stations have been relevant issues in applying the open-water method to systems influenced by physical mixing (Russell and Montagna 2007, Staehr et al. 2010). Application of the method to estuaries is a particular concern as physical mixing caused by tidal currents may confound the biological variation in DO time series (Kemp and Boynton 1980, Caffrey 2003, Nidzieko et al. 2014). Individual sampling stations near bay inlets or along major tidal axes may produce DO time series that fail to meet the assumptions of the open-water method.

Although numerous studies have shown that application of the open-water method to lakes or estuaries may be problematic (Ziegler and Benner 1998, Caffrey 2003, Coloso et al. 2011, Batt and Carpenter 2012, Nidzieko et al. 2014), very few quantitative approaches have been developed to address potential bias or noise in DO signals from physical advection. For example, an

extensive analysis by Caffrey (2003) applied the open-water method to estimate metabolism at 28 continuous monitoring stations at 14 US estuaries. A significant portion of the production and respiration estimates were negative (3 - 69% depending on site), suggesting advection of water masses was a likely factor influencing the DO time series. These ‘anomalous’ values are typically omitted from the analysis (Caffrey 2003, Collins et al. 2013), which may upwardly bias estimates of metabolism (Murrell et al. 2013). Further, Nidzieko et al. (2014) evaluated the effects of tidal advection on metabolism estimates in a mesotidal estuary. Estimates from a single location were strongly correlated with the spring-neap cycle such that net heterotrophy was more common during spring tides, whereas metabolism was generally balanced during neap tides. A control-volume approach was used by impounding a section of the upper estuary to understand how physical processes contribute to biological variability. Although useful as an *in situ*, site-specific approach, more accessible statistical methods specific to time series are needed given the increasing availability of continuous monitoring data. For example, Batt and Carpenter (2012) explored the use of a Kalman filter (Harvey 1989) to remove process and observation uncertainty from DO time series in lakes. Similar approaches have not been developed for estuaries, particularly those that address potential effects of tidal advection.

This article describes the development and application of a method for improving estimates of ecosystem metabolism computed from DO time series. Specifically, the apparent effects of tidal advection on DO observations are removed to improve the fidelity of open-water metabolism estimates derived from continuous water quality data. We used a weighted regression approach originally developed to resolve trends in pollutant concentrations in streams and rivers (Hirsch et al. 2010). The weighted regression approach creates dynamic predictions of DO as a function of time and tidal height change, which are then used to filter, or detide, the DO signal.

The model is based on the recognition that daily fluctuations in DO are caused by metabolism associated with the solar cycle, whereas other fluctuations in estuaries are likely associated with water level changes that generally exhibit precession relative to the solar cycle. The weighted regression model was applied, rather than methods commonly used for detiding in physical oceanography, to allow for the complex and dynamic patterns of DO changes relative to advection. First, we used simulated DO time series with known characteristics to evaluate ability of the weighted regression to remove the simulated effects of a tidally-advected DO gradient. Second, the simulation results informed the application of the method to four case studies chosen from the National Estuarine Research Reserve System (NERRS, [Wenner et al. 2004](#)). In all examples, tidal height is used as a proxy for lateral water movements that may influence DO observations. In the absence of quantitative data describing lateral DO variation (e.g., contemporaneous stations along a tidal axis), we assume tidal height is an appropriate characterization of lateral variation. Accordingly, ‘tidal variation’ or ‘changes in tidal height’ are used throughout in reference to assumed lateral DO gradients that are carried past monitoring sensors by tidal currents.

Materials and Procedures

Weighted regression for modelling and filtering DO time series

For this study, we adapted a weighted regression model to filter DO time series for apparent tidal effects. This model relied heavily on concepts used to develop the weighted regression on time, discharge, and season (WRTDS) method for estimating pollutant

{acro:WRTDS}

118 concentrations in streams and rivers (Hirsch et al. 2010). The functional form of the model is:

$$DO_{obs} = \beta_0 + \beta_1 t + \beta_2 H \quad (1) \quad \{\text{funform}\}$$

119 where DO_{obs} is a linear function of time t and tidal height H . Time is a continuous variable for
120 the day and time of each observation as a proportion of the number of total observations added to
121 each day. The beginning of each day was considered the nearest thirty minute observation to
122 sunrise for the location. Our model differed from the original WRTDS method that included
123 parameters to estimate variation of the response variable on a sinuisoidal period. DO variation
124 was not modeled using this approach to avoid constraining parameter estimates by periodic, diel
125 components.

126 Weighted regression was implemented as a moving window that allowed for estimation of
127 DO throughout the time series by adapting to variation through time as a function of tide.
128 Regression models were estimated sequentially for each observation in the time series using
129 dynamic weight vectors that change with the center of the window. Weight vectors quantified the
130 relevance of observations to the center of the window in respect to time, hour of the day, and tidal
131 height. Specifically, weights were assigned to each variable using a tri-cube weighting function
132 (Tukey 1977, Hirsch et al. 2010):

$$w = \begin{cases} \left(1 - (d/h)^3\right)^3 & \text{if } |d| \leq h \\ 0 & \text{if } |d| > h \end{cases} \quad (2)$$

133 where the weight w of each observation is inversely proportional to the distance d from the center
134 of the window such that observations more similar to the point of reference are given higher

importance in the regression. Weights exceeding the maximum width of the window h are equal to zero. The tri-cube weighting function is similar to a Gaussian distribution such that weights decrease gradually from the center until the maximum window width is reached. Regressions that use simpler windows (e.g., boxcar approach) are more sensitive to influential observations as they enter or leave the window, whereas the tri-cube function minimizes their effect through gradual weighting of observations from the center ([Hirsch et al. 2010](#)). The final weight vector for each observation is the product of three separate weight vectors for time (day), hour, and tidal height. Windows for time and hour weight observations based on distance (time) from the center of the window. The window for tidal height weights observations based on the difference from the center as a proportion of the total tidal height range. For example, a half-window width of 0.5 means that observations are weighted proportionately within +/- 50% the total range referenced to the tidal height in the center of the window. A low weight is given to an observation if any of the three weighting values were not similar to the center of the window since the final weight vector is the product of three weight vectors for each variable (see the link in the [multimedia](#) section for graphical display of different weights).

The choice of window widths for weight vectors strongly affects the model results. Excessively large or small window widths may respectively under- or over-fit the observed data. Accordingly, appropriate window widths depend on the objective for using the model. The weighted regression approach can be used for both predicting observed DO and filtering the observed time series to remove the variance that coincided with the tidal cycle. Window widths that minimize prediction error or fit to the observed data are typically smaller than widths that would be used for filtering tidal effects. Similarly, window widths that more effectively filter the DO signal may produce imprecise predictions for the observed data. Evaluations of the weighted

regression method with simulated DO time series, described below, used multiple window widths to evaluate the ability of the model to filter the DO signal. The ability to predict observed DO was not a primary objective such that the window widths were evaluated only in the context of removing tidal variation from the DO time series.

The approach to filter physical advection from the observed DO time series differs slightly from methods in [Hirsch et al. \(2010\)](#). The previous approach used a two-dimensional grid predicted for stream pollutant concentrations across the time series and the range of discharge values observed in the study system ([Hirsch et al. 2010](#)). Normalized or discharge-independent values for pollutant concentration were obtained by averaging grid predictions across the discharge values that were likely to occur on a given day. Rather than creating a two-dimensional grid of DO related to time and tidal height change, the normalized time series herein were the model predictions conditional on time and constant tidal height set to the mean:

$$DO_{nrm} = f(DO_{obs} | \bar{H}, t) \quad (3) \quad \{do_nrm\}$$

such that the normalized time series represents DO variation related to biological processes. The term ‘filter’ is used in reference to the removal of a specific variance component from the time series, while maintaining the structure of the biological component. Although the approach shares similarities with common filtering techniques, a distinction is noted such that weighted regression has a specific purpose rather than the more generic objectives of common filters (e.g., moving window averages or local smoothers, [Shumway and Stoffer 2011](#)).

Assessment

Simulation of DO time series

To test the ability of the weighted regression to filter the DO signal for apparent tide effects, multiple time series with known characteristics were simulated and filtered. A simulation approach was used prior to application with real data given that the true biological signal can be created as a known component for comparison with the filtered results from weighted regression. The following describes the theoretical basis for developing the simulated time series. Observed DO time series were simulated as the sum of variation from biological processes and physical effects related to tidal advection:

$$DO_{obs} = DO_{bio} + DO_{adv} \quad (4) \quad \{do_obs\}$$

Biological DO signals are inherently noisy (Batt and Carpenter 2012) and variance can be further described as:

$$DO_{bio} = DO_{die} + DO_{unc} \quad (5) \quad \{do_bio\}$$

$$DO_{unc} = \epsilon_{obs} + \epsilon_{proc} \quad (6) \quad \{do_unc\}$$

where the biological DO signal (DO_{bio}) is the sum of diel variation (DO_{die}) plus uncertainty or noise (DO_{unc}). Total uncertainty in the biological DO signal is described as variation from observation and process uncertainty (ϵ_{obs} and ϵ_{proc} , Hilborn and Mangel 1997). Multiple time series at 30 minute time steps over 30 days were created by varying the relative magnitudes of each of the components of observed DO in eqs. (4) to (6) to test the effectiveness of weighted

193 regression under different scenarios. Accordingly, observed DO was generalized as the additive
 194 combination of four separate time series (Fig. 1):

$$DO_{obs} = DO_{adv} + DO_{die} + \epsilon_{obs} + \epsilon_{pro} \quad (7) \quad \{\text{do_obs_a}\}$$

195 Each component of the simulated time series was created as follows. First, the diel
 196 component, DO_{die} , was estimated (Cryer and Chan 2008):

$$DO_{die} = \alpha + \beta \cos(2\pi ft + \Phi) \quad (8) \quad \{\text{do_sin}\}$$

197 such that the mean DO (α) was 8, amplitude (β) was 1, f was 1/48 to represent 30 minute
 198 intervals, t was the time series vector and Φ was the x-axis origin set for an arbitrary sunrise at
 199 630. The diel signal was increasing during the day and decreasing during the night for each 24
 200 hour period and ranged from 7 to 9 mg L⁻¹. Uncertainty was added to the diel DO signal as the
 201 sum of observation and process uncertainty:

$$DO_{unc,n} = \epsilon_{obs,n} + \int_{t=1}^n \epsilon_{pro,t} \quad (9) \quad \{\text{do_unc_n}\}$$

202 where observation and process uncertainty (ϵ_{obs} , ϵ_{pro}) were simulated as normally distributed
 203 random variables with mean zero and standard deviation varying from zero to an upper limit,
 204 described below. Process uncertainty was estimated as a serially correlated variable using the
 205 cumulative sum of n observations plus random variation added at each time step for $t = 1, \dots, n$.
 206 The total uncertainty, DO_{unc} , was added to the diel DO time series to create the biological DO
 207 time series (eq. (5) and Fig. 1).

A semidiurnal tidal series was simulated with a period of 12.5 hours to represent the principal lunar component (Foreman and Henry 1989). The amplitude was set to 1 meter and centered at 4 meters. The tidal time series simulated DO changes with advection, DO_{adv} (eq. (7) and Fig. 1). Conceptually, this vector represents the rate of change in DO as a function of horizontal water movement from tidal advection such that:

$$\frac{\delta DO_{adv}}{\delta t} = \frac{\delta DO}{\delta x} \cdot \frac{\delta x}{\delta t} \quad (10) \quad \{\text{deltado}\}$$

$$\frac{\delta x}{\delta t} = k \cdot \frac{\delta H}{\delta t} \quad (11) \quad \{\text{deltx}\}$$

where the first derivative of the tidal time series, as change in height over time $\delta H/\delta t$, is multiplied by a constant k , to estimate horizontal tidal excursion over time, $\delta x/\delta t$. The horizontal excursion is assumed to be associated with a horizontal DO change, $\delta DO/\delta x$, such that the product of the two estimates the DO change at each time step from advection, DO_{adv} . In practice, the simulated tidal signal was used to estimate DO_{adv} :

$$DO_{adv} \propto H \quad (12) \quad \{\text{do_adv}\}$$

$$DO_{adv} = 2 \cdot a + a \cdot \frac{H - \min H}{\max H - \min H} \quad (13) \quad \{\text{do_adv}\}$$

where a is analogous to k in eq. (11) and is chosen as the transformation parameter to standardize change in DO from tidal height change to desired units. For example, $a = 1$ will convert H to a scale that simulates changes in DO from tidal advection that range from +/- 1 mg L⁻¹. The final time series for observed DO was the sum of biological DO and advection DO (eq. (4) and Fig. 1).

Evaluation of weighted regression with simulated DO time series

Multiple time series were simulated by varying the conditions in eq. (7) ((Fig. 2)) to evaluate weighted regression under difference conditions. Specifically, the simulated data varied in the relative amount of noise in the measurement (e_{pro} , e_{obs}), relative amplitude of the diel DO component (DO_{die}), and degree of association of the tide with the DO signal (DO_{adv}). Three levels were evaluated for each variable: relative noise as 0, 1, and 2 standard deviations for both process and observation uncertainty, amplitude of diel biological DO as 0, 1, and 2 mg L⁻¹, and DO change from tidal advection as 0, 1, and 2 mg L⁻¹. A total of 81 time series were created based on the unique combinations of parameters (Fig. 2). Half-window widths (day, hour of day, and tide height) for the weighted regressions were evaluated for each time series: time as 1, 3, and 6 days, time of day as 1, 3, and 6 hours, and tidal height as 0.25, 0.5, and 1 as a proportion of the total range given the height at the center of the window. The window widths were chosen based on preliminary assessments that suggested a large range in model performance was described by these values. In total, 27 window width combinations were evaluated for each of 81 simulated time series, producing results for 2187 weighted regressions.

The filtered DO time series were compared to the simulated data to evaluate the ability of weighted regression to characterize the biological DO time series in eq. (4). Comparisons were made using Pearson correlation coefficients and the root mean square error (RMSE). Overall, the weighted regressions produced filtered time series that were similar to the ‘true’ biological time series regardless of the simulation parameters (Table 1) or window widths (Table 2, results for each simulation can be viewed using the link in the [multimedia](#) section). The median correlation between the filtered and biological values for all time series and window widths was 0.59, with

{acro:RMSE}

values ranging from -0.78 (very poor) to 1.00 (perfect). Mean error was 1.10, with values ranging from 0 (perfect) to 2.40 (very poor). Simulations with very poor performance were those that had minimum widths for day windows and maximum widths for hour windows, or were those with the DO signal composed entirely of noise from observation uncertainty. As expected, simulations with no biological or tidal influence had filtered time series that were identical to the true time series (e.g., correlation of one, RMSE of zero).

Characteristics of DO time series that contributed to improved model performance were increasing amplitude of the diel DO component (DO_{die}) and increasing process error (e_{pro}), whereas increasing observation error contributed to decreased performance (Table 1 and Fig. 3). Model performance decreased slightly with increasing tidal effects (i.e., increasing magnitude of DO_{adv}). Increasing widths for day and tidal height windows contributed to improved model performance, whereas reduced performance was observed with increasing hour windows (Table 2 and Fig. 4). Graphical summaries of model performance by simulation parameters (Fig. 3) and half window widths (Fig. 4) support the general trends described by Tables 1 and 2.

Validation of weighted regression with case studies

Results from the simulated time series were used to inform the validation of weighted regression with real data, specifically with respect to choosing half-window widths described below. Continuous monitoring data from the National Estuarine Research Reserve System was used to validate the weighted regression model by evaluating estimates of ecosystem metabolism obtained from observed and filtered DO time series. NERRS is a federally-funded network of 28 protected estuaries established for long-term research, water-quality monitoring, education, and coastal stewardship (Wenner et al. 2004). Continuous water quality data have been collected at

NERRS sites since 1994 through the System Wide Monitoring Program (SWMP, [CDMO 2014](#)).

In addition to providing a basis for trend evaluation, data from SWMP provides an ideal opportunity to evaluate long-term variation in water quality parameters from biological and physical processes. Continuous SWMP data can be used to describe DO variation at sites with different characteristics, including variation from ranges in tidal regime ([Sanger et al. 2002](#)) and rates of ecosystem production ([Caffrey 2003, 2004](#)). We selected sites from the SWMP database that had desirable characteristics for validating weighted regression. Specifically, four macrotidal sites were chosen based on apparent relationships between DO and tidal changes (Fig. 5 and Table 3): Vierra Mouth station at Elkhorn Slough (California, 36.81°N, 121.78°W), Bayview Channel at Padilla Bay (Washington, 48.50°N 122.50°W), Middle Blackwater River station at Rookery Bay (Florida, 25.93°N 81.60°W), and Dean Creek station at Sapelo Island (Georgia, 31.39°N 81.28°W).

The weighted regression model was applied to continuous DO time series and water level measurements from January 1st to December 31st 2012 at the four sites. Tide predictions were obtained for each site using harmonic regression applied to the sonde depth data (`oce` package in R, [Foreman and Henry 1989, RDCT 2014](#)). The stations were generally semidiurnal or mixed semidiurnal and net heterotrophic on an annual basis (Table 3). Net heterotrophy (i.e., respiration exceeding production) is typical for shallow water systems at temperate latitudes ([Caffrey 2003](#)), although values in Table 3 were from observed DO time series that were strongly correlated with water level height.

Estimates of ecosystem metabolism before and after filtering

{met_sec}

The weighted regression method was applied to the annual data for each station to obtain a filtered DO time series for estimating metabolism. Ecosystem metabolism was estimated using the open-water technique (Odum 1956) as described in Caffrey et al. (2013). The method is used to infer net ecosystem metabolism using the mass balance equation:

$$\frac{\delta DO}{\delta t} = P - R + D \quad (14) \quad \{\text{metrate}\}$$

where the change in DO concentration (δDO , g O₂ m⁻³) over time (δt , hours) is equal to photosynthetic rate (P , g O₂ m⁻³ hr⁻¹) minus respiration rate (R , g O₂ m⁻³ hr⁻¹), corrected for air-sea gas exchange (D , g O₂ m⁻³ hr⁻¹) (Caffrey et al. 2013). D is estimated as the difference between the DO saturation concentration and observed DO concentration, multiplied by a volumetric reaeration coefficient, k_a (Thébault et al. 2008). The diffusion-corrected DO flux estimates were averaged during day and night for each 24 hour period in the time series, where flux is an hourly rate of DO change. Respiration rates were assumed constant during the night and subtracted from daily net production estimates to yield gross production (Table 3).

Half window widths of six days, one hour, and a tidal proportion of one half were used to filter the observed DO time series. Although the selection of window widths involves a degree of subjectivity, results from the simulations suggested that these values were appropriate for filtering DO times series within the constraints of the analysis. Unlike the simulated data, the true biological DO signal was unknown for the case studies. Accordingly, the regression results were evaluated using correlations of DO and metabolism estimates with tidal height before and after application of the model. Daily metabolism estimates before and after filtering were compared to

the mean rate of tidal height change (i.e., first derivative of the predicted tidal height) for each day during separate solar periods. Production rates were compared to mean rates of tidal height change during the day, respiration rates were compared to mean rates of change during the night, and net metabolism rates were compared to mean rates of change for the total 24 hour period each day. Results were also evaluated based on the occurrence of ‘anomalous’ daily production or respiration estimates, where anomalous was defined as negative production during the day and positive respiration estimates during the night. Anomalous values have been previously attributed to the effects of physical processes on DO time series (Caffrey 2003). Although anomalies could be caused by processes other than tidal advection, e.g., abiotic dark oxygen production (Pamatmat 1997), we assumed that physical processes were the dominant sources of these values given the tidal characteristics at each site. Finally, means and standard errors of metabolism estimates were evaluated before and after filtering to determine if annual aggregations were significantly different.

Filtering had significant effects on the correlations between water level changes, DO time series, and daily integrated metabolism estimates (Table 4, see the link in the multimedia section for graphical results of each case study). Correlations of observed DO time series with predicted tidal height were highly significant and positive at all sites, except Padilla Bay where increases in water level were associated with decreases in DO concentration. The filtered DO time series had greatly reduced correlations with tidal height, although relationships were still significant after filtering likely because of the large sample size for each site ($n \approx 17,500$). Comparison of metabolic rates to tidal changes before and after filtering produced inconsistent results (Table 4). Correlations for Elkhorn Slough and Sapelo Island showed consistent reductions in all three metabolisms estimates after filtering. Correlations for Padilla Bay and Rookery Bay were of

opposite sign and greater magnitude after filtering for production and respiration, although net metabolism estimates had reduced correlations.

The proportion of daily integrated metabolism estimates that were anomalous (negative production, positive respiration) were significantly reduced for most sites after filtering (Table 5), perhaps indicating the relative effects of water movement. Before filtering, anomalous values ranged from 0.09 (as a proportion of the total estimates, Rookery Bay) to 0.22 (Padilla Bay) for production and 0.08 (Rookery Bay) to 0.21 (Elkhorn Slough) for respiration. Anomalous values were reduced to near zero for Rookery Bay and Sapelo Island, by approximately half for Padilla Bay (0.08, 0.07, 0.06, 0.06, 0.07, 0.08, 0.10, 0.11, 0.07, 0.06, 0.06, 0.08, 0.14, 0.08, 0.09, 0.06, 0.05, 0.05, 0.06, 0.14, 0.06, 0.04, 0.04, 0.06, 0.06, 0.18, 0.08, 0.04, 0.05, 0.06, 0.04, 0.05, 0.06, 0.28, 0.10, 0.06, 0.06, 0.07, 0.06, 0.35, 0.16, 0.08, 0.07, 0.06, 0.05, 0.07, 0.12, 0.08, 0.06, 0.04, 0.07, 0.07, 0.06, 0.06, 0.06, 0.12, 0.05, 0.04, 0.05, 0.07, 0.06, 0.16, 0.07, 0.05, 0.04, 0.05, 0.22, 0.11, 0.05, 0.05, 0.08, 0.06, 0.05, 0.08, 0.13, 0.14, 0.15, 0.06, 0.06, 0.07, 0.07, 0.07, 0.06, 0.11, 0.05, 0.06, 0.06, 0.06, 0.15, 0.08, 0.04, 0.04, 0.04, 0.05, 0.17, 0.10, 0.04, 0.04, 0.06, 0.05, 0.07, 0.10, 0.11, 0.06, 0.14, 0.07, 0.06, 0.08, 0.08, 0.07, 0.08, 0.07, 0.05, 0.05, 0.06, 0.06, 0.14, 0.07, 0.04, 0.04, 0.06, 0.18, 0.09, 0.04, 0.04 for production, 0.07, 0.07, 0.06, 0.06, 0.06, 0.08, 0.10, 0.11, 0.08, 0.06, 0.06, 0.08, 0.19, 0.07, 0.09, 0.06, 0.05, 0.05, 0.06, 0.12, 0.06, 0.04, 0.04, 0.06, 0.06, 0.19, 0.08, 0.04, 0.05, 0.06, 0.04, 0.05, 0.06, 0.33, 0.11, 0.06, 0.05, 0.07, 0.06, 0.39, 0.20, 0.08, 0.07, 0.06, 0.06, 0.07, 0.12, 0.08, 0.06, 0.04, 0.08, 0.07, 0.06, 0.06, 0.06, 0.14, 0.04, 0.04, 0.06, 0.07, 0.07, 0.21, 0.06, 0.04, 0.04, 0.05, 0.34, 0.12, 0.04, 0.04, 0.08, 0.06, 0.06, 0.07, 0.12, 0.13, 0.15, 0.07, 0.07, 0.07, 0.06, 0.07, 0.06, 0.11, 0.06, 0.06, 0.06, 0.06, 0.17, 0.07, 0.04, 0.04, 0.04, 0.06, 0.25, 0.11, 0.04, 0.05, 0.06, 0.06, 0.07, 0.10, 0.10, 0.06, 0.14, 0.07, 0.07, 0.07, 0.09, 0.08, 0.09, 0.07, 0.05, 0.05, 0.07, 0.07, 0.12, 0.08, 0.04, 0.04, 0.06, 0.20, 0.10, 0.04, 0.04 for

respiration), and only slightly reduced for Elkhorn Slough (0.18, 0.07, 0.05, 0.22, 0.24, 0.19,
 0.18, 0.16, 0.15, 0.21, 0.19, 0.13, 0.18, 0.13, 0.16, 0.15, 0.12, 0.09, 0.05, 0.18, 0.13, 0.10, 0.05,
 0.14, 0.03, 0.20, 0.12, 0.10, 0.05, 0.02, 0.10, 0.08, 0.08, 0.26, 0.17, 0.12, 0.09, 0.16, 0.09, 0.33,
 0.21, 0.14, 0.13, 0.13, 0.21, 0.20, 0.16, 0.13, 0.15, 0.11, 0.15, 0.15, 0.15, 0.11, 0.11, 0.18, 0.16,
 0.12, 0.09, 0.14, 0.08, 0.18, 0.16, 0.12, 0.09, 0.08, 0.23, 0.18, 0.12, 0.08, 0.13, 0.11, 0.22, 0.23,
 0.17, 0.14, 0.13, 0.16, 0.18, 0.16, 0.13, 0.16, 0.09, 0.16, 0.16, 0.12, 0.11, 0.08, 0.16, 0.15, 0.12,
 0.07, 0.13, 0.07, 0.19, 0.15, 0.12, 0.08, 0.07, 0.22, 0.23, 0.17, 0.18, 0.10, 0.15, 0.15, 0.19, 0.18,
 0.14, 0.11, 0.16, 0.17, 0.12, 0.10, 0.07, 0.07, 0.16, 0.15, 0.11, 0.07, 0.05, 0.19, 0.13, 0.11, 0.07 for
 production, 0.19, 0.05, 0.06, 0.24, 0.23, 0.18, 0.18, 0.16, 0.19, 0.24, 0.21, 0.13, 0.21, 0.10, 0.15,
 0.18, 0.13, 0.10, 0.06, 0.19, 0.14, 0.10, 0.06, 0.15, 0.04, 0.23, 0.14, 0.10, 0.06, 0.03, 0.11, 0.08,
 0.08, 0.30, 0.18, 0.14, 0.10, 0.15, 0.09, 0.36, 0.22, 0.14, 0.11, 0.11, 0.24, 0.20, 0.16, 0.11, 0.15,
 0.11, 0.16, 0.16, 0.16, 0.11, 0.09, 0.17, 0.17, 0.13, 0.09, 0.13, 0.08, 0.23, 0.16, 0.13, 0.09, 0.08,
 0.29, 0.18, 0.12, 0.09, 0.13, 0.08, 0.24, 0.23, 0.16, 0.15, 0.13, 0.18, 0.19, 0.16, 0.12, 0.18, 0.09,
 0.16, 0.17, 0.13, 0.12, 0.08, 0.20, 0.15, 0.13, 0.08, 0.14, 0.07, 0.27, 0.16, 0.11, 0.09, 0.07, 0.24,
 0.23, 0.17, 0.18, 0.09, 0.15, 0.19, 0.22, 0.18, 0.14, 0.10, 0.16, 0.17, 0.13, 0.11, 0.07, 0.07, 0.16,
 0.14, 0.11, 0.07, 0.05, 0.25, 0.15, 0.11, 0.07 for respiration). Metabolism estimates using filtered
 DO time series had decreased mean production (-69.3 % change from the annual mean) and
 respiration (-69.3 %) for Elkhorn Slough, increased mean production (43.7 %) and respiration
 (44.7 %) for Padilla Bay, and generally unchanged mean production and respiration for Rookery
 Bay and Sapelo Island (Table 5). Mean net ecosystem metabolism was unchanged for all sites.
 Decreases in the standard error for all metabolism estimates (production, respiration, and net)
 were observed for all cases after filtering.

An example from Sapelo Island illustrates the effects of weighted regression on DO and

metabolism estimates (Figs. 6 to 8). A two-week period in February showed when the tidal cycles were both in and out of phase with the diel cycling, where phasing describes synchronicity between maximum tide heights and day/night periods (Nidzieko et al. 2014). That is, maximum tide heights were generally out of phase with the diel cycle during the first week when low tides were observed during the middle of the night and the middle of the day (Fig. 6), whereas tide heights were in phase during the second week when the maximum tide height occurred during the day and night (Fig. 7). The effects of tidal height change on the observed DO time series are visually apparent in the plots. The first week illustrates a strong negative bias (less respiration, less production) in the observed DO signal from low tides at mid-day and mid-night, whereas the second example illustrates a strong positive bias (more respiration, more production) in the observed DO from high tides. These biases are apparent in the metabolism estimates using the observed data (Fig. 8). Anomalous estimates occur when low tides are in phase with the solar cycle (week one), whereas metabolism estimates are likely over-estimated when high tides are in phase with the solar cycle (week two). The filtered time series shows noticeable changes given the direction of bias from the phasing between tidal height and diel period. DO values were higher after filtering when low tides occurred during night and day periods, whereas DO values were lower after filtering when high tides occurred during day and night periods (Figs. 6 and 7). Changes in metabolism estimates after filtering were also apparent, such that the anomalous values were removed during the first week and the positive bias in the second week is decreased (Fig. 8).

Effects of aggregation and importance of filtering

A point of concern is the period of observation within which observed DO is affected by tidal height changes and the extent to which this affects the interpretation of ecosystem metabolism. The effects of tidal variation on daily estimates may not be relevant if seasonal or annual aggregations (e.g., mean annual metabolism) remove this potential bias. The example from Sapelo Island in the previous section highlights this point given that mean production and respiration estimates before and after filtering were generally unchanged for the two-week period. Alternatively, annual averages of production and respiration estimates were significantly different for Elkhorn Slough and Padilla Bay (Table 5). Given these results, tidal variation may or may not have effects on metabolism estimates on aggregated time scales, depending on the location. Therefore, an evaluation of weighted regression to filter the effects of tidal variation on ecosystem metabolism for different periods of observation is critical for its application. Specifically, when should filtering be applied if aggregation of observed data on longer time periods removes potential bias? A comparison of observed and filtered estimates that are aggregated over different periods of observation could help address this question.

The observed and filtered daily estimates were averaged by month for each case study to evaluate effects of aggregation on mean production and respiration. Mean annual estimates in Table 5 also provided a basis of comparison with the aggregations. Significant variation in aggregated production and respiration estimates was observed for each case study (Fig. 9). Filtered production and respiration estimates for Padilla Bay and Rookery Bay exhibited monthly variation that was more characteristic of expected trends during warmer months. Specifically, metabolism estimates based on observed DO were substantially muted for both Padilla Bay and

Rookery Bay during summer months, whereas values were significantly higher after filtering. Results for Sapelo Island suggested that aggregated estimates were similar before and after filtering, although winter and summer months were slightly under- and over-estimated, respectively, using the observed data. Results for Elkhorn Slough varied significantly such that production and respiration were significantly reduced after filtering. Overall, these trends emphasize the importance of considering different aggregation periods for interpreting metabolism estimates. Each case study showed differences in observed and filtered values at monthly aggregations, whereas only two of the four case studies had mean aggregated estimates that were substantially different (Elkhorn Slough and Padilla Bay, Table 5). Periods of observation as long as one year may include significant sources of bias from tidal advection, suggesting the need for applying weighted regression given careful consideration of appropriate window widths.

Discussion

The weighted regression approach was developed to improve estimates of ecosystem metabolism by removing variation associated with tidal change in observed DO time series. The application to simulated DO time series with known characteristics and extension to continuous monitoring data from selected NERRS sites suggested the approach can isolate and remove variation in observed DO from tidal change. Further, aggregation of metabolism estimates using the filtered DO time series were significantly different than those using the observed data, particularly for relatively long periods of observation depending on location. These results suggest that previous estimates of annual means may not accurately reflect true metabolic signals if the effects of tidal variation confound biological signals in observed DO time series. Additionally, variation of aggregated metabolism estimates were substantially reduced after

441 filtering, suggesting greater confidence in interpreting estimates even if the mean values are
442 similar.

443 Comparisons between filtered and biological DO time series from the simulations
444 indicated that weighted regression can reduce the effects of tidal variation for a range of
445 characteristics of DO time series. An examination of scenarios that produced abnormal results
446 can provide additional insight into factors that affect the performance of weighted regression. For
447 example, poor performance was observed when the observation uncertainty (ϵ_{obs}) was high and
448 both process uncertainty (ϵ_{pro}) and tidal advection (DO_{adv}) were low. These examples represent
449 time series with excessive random variation, no auto-correlation, and no tidal influence. Poor
450 performance is expected because the weighted regression models a non-existent tidal signal in a
451 very noisy DO time series. These results were observed even for time series with a large diel
452 component of the biological DO signal, suggesting that the model will produce random results in
453 microtidal systems with high noise and no serial correlation. From a practical perspective,
454 weighted regression should not be applied to noisy time series if there is not sufficient evidence to
455 suggest the variation is related to tidal changes. Alternative approaches, such as the Kalman filter
456 (Harvey 1989, Batt and Carpenter 2012), may be more appropriate if random variation is the
457 primary source of uncertainty. Similarly, results with perfect or near-perfect correlations between
458 filtered and biological DO time series were observed when observation uncertainty and tidal
459 effects were not components of the simulated time series. Although there is no need to apply
460 weighted regression to time series with no apparent tidal influences, the results will not be
461 incorrect. We emphasize that the weighted regression should only be applied to time series for
462 which specific conditions apply, as described in the recommendations below.

463 Correlations of metabolism estimates with tidal height changes after filtering were

generally reduced, although trends were not always consistent. However, correlations of net metabolism estimates were reduced in all cases. An additional indication of the effectiveness of weighted regression was the reduction of anomalous metabolism estimates after filtering for all case studies. Negative production and positive respiration estimates suggest assumptions of the open-water method are violated (Needoba et al. 2012), although ‘normal’ estimates (positive production and negative respiration) may still include a significant source of bias from physical advection by providing over-estimates of true values. For example, Nidzieko et al. (2014) observed that net metabolism at Elkhorn Slough was strongly heterotrophic during spring tides that occurred at nighttime such that inundation of salt marshes during the night following by draining with low tide during the day lead to inflated respiration values. Synchrony between solar and tidal cycles is a critical concern for interpreting metabolism estimates, although a broader discussion regarding whether or not this represents an actual bias in metabolism from physical advection may be needed.

The weighted regression approach makes no assumptions as to the relationships between DO and tidal variation over time. Although the functional form of the model is a simple linear regression with only two explanatory variables (eq. (1)), the moving window approach combined with the adaptive weighting scheme allows for quantification of complex tidal effects that may not be possible using alternative approaches. A similar approach by Batt and Carpenter (2012) uses a Kalman filter to improve estimates of ecosystem metabolism in lakes. The approach minimizes uncertainty in observed DO using a filter that combines information about the data generation process and the manner in which the data are observed (Harvey 1989). Although a similar approach could be used for estuaries, it may not be effective given that the effects of tidal advection are not related to process or observation uncertainty. Additionally, results from the case

studies illustrated the ability of the weighted regression approach to model changes over time in the relationships between tidal change and DO. Results for Padilla Bay and Rookery Bay suggested that filtering had the largest effect during the summer, whereas the results for cooler months were not significantly different from the observed. The weighted regression method produced filtered time series that accommodated seasonal variation in DO conditional on tidal height change, whereas moving window filters or standard regression techniques would likely not have characterized these dynamic relationships.

Comments and recommendations

Results from the simulations and case studies suggested that weighted regression can be a practical approach for filtering DO time series to remove the effects of physical advection on estimates of ecosystem metabolism. However, application of the method may only be appropriate under specific situations. The case studies were chosen based on the relatively high proportion of metabolism estimates that were anomalous and the strength of correlation between the observed DO time series and tidal height. Despite these similarities among the case studies, filtering had variable effects on metabolism estimates. The results for Elkhorn Slough and Padilla Bay are of particular concern given that mean annual estimates were substantially different compared to those from the observed DO time series. Although the correlation of DO and tidal height was reduced for both cases, in addition to a reduction of anomalous estimates, the relative change in mean metabolism before and after filtering suggests a more careful evaluation of the method is needed. In particular, alternative window widths should be evaluated for the ability to remove tidal effects while preserving the biological signal. The window widths in the above analysis may have removed variation in the DO signal from both of these sources.

Although the above analyses suggest the approach has merit, the case studies emphasize a critical challenge in applying weighted regression to monitoring data. Specifically, the true biological signal is not known and the relative contribution of horizontal advection to bias is not accurately quantified with the available data. Comparative analyses between systems with varying tidal influence or within-system evaluations of multiple sites at fixed distances are necessary to further validate the performance of weighted regression. In the absence of additional validation, we propose a precautionary approach for application of the weighted regression to monitoring data. Weighted regression may be most effective at macrotidal sites with strong evidence of the effects of tidal advection on biological signals. A weight-of-evidence approach should be used such that the occurrence of anomalous metabolism estimates, strong correlations between observed DO and tide height, and clear visual patterns of tide change on DO would suggest filtering is appropriate. The choice of window widths may also produce varying results. Window widths that produce large changes in mean annual estimates should be interpreted with caution. In general, a pragmatic approach is emphasized such that results should be evaluated based on the preservation of diel variation from production while exhibiting minimal changes with the tide. Such an approach, combined with further validation, will support informed management decisions through more accurate estimates of ecosystem metabolism.

References

- Batt RD, Carpenter SR. 2012. Free-water lake metabolism: Addressing noisy time series with a Kalman filter. *Limnology and Oceanography: Methods*, 10:20–30.
- Caffrey JM. 2003. Production, respiration and net ecosystem metabolism in U.S. estuaries. *Environmental Monitoring and Assessment*, 81(1-3):207–219.
- Caffrey JM. 2004. Factors controlling net ecosystem metabolism in U.S. estuaries. *Estuaries*, 27(1):90–101.
- Caffrey JM, Murrell MC, Amacker KS, Harper J, Phipps S, Woodrey M. 2013. Seasonal and inter-annual patterns in primary production, respiration and net ecosystem metabolism in 3 estuaries in the northeast Gulf of Mexico. *Estuaries and Coasts*.
- CDMO (Centralized Data Management Office). 2014. National Estuarine Research Reserve System. <http://cdmo.baruch.sc.edu/>. (Accessed January, 2014).
- Cloern JE. 1996. Phytoplankton bloom dynamics in coastal ecosystems: A review with some general lessons from sustained investigation of San Francisco Bay, California. *Review of Geophysics*, 34(2):127–168.
- Collins JR, Raymond PA, Bohlen WF, Howard-Strobel MM. 2013. Estimates of new and total productivity in Central Long Island Sound from in situ measurements of nitrate and dissolved oxygen. *Estuaries and Coasts*, 36(1):74–97.
- Coloso JJ, Cole JJ, Pace ML. 2011. Difficulty in discerning drivers of lake ecosystem metabolism with high-frequency data. *Ecosystems*, 14(6):935–948.
- Cryer JD, Chan KS. 2008. *Time Series Analysis with Applications in R*. Springer, New York, New York, second edition.
- Diaz RJ, Rosenberg R. 2008. Spreading dead zones and consequences for marine ecosystems. *Science*, 321:926–929.
- Foreman MGG, Henry RF. 1989. The harmonic analysis of tidal model time series. *Advances in Water Resources*, 12(3):109–120.
- Harvey AC. 1989. *Forecasting, Structural Time Series Models and the Kalman Filter*. Cambridge University Press, Cambridge, United Kingdom.
- Hilborn R, Mangel M. 1997. *The Ecological Detective: Confronting Models with Data*. Princeton University Press, Princeton, New Jersey.
- Hirsch RM, Moyer DL, Archfield SA. 2010. Weighted regressions on time, discharge, and season (WRTDS), with an application to Chesapeake Bay river inputs. *Journal of the American Water Resources Association*, 46(5):857–880.

- Kemp WM, Boynton WR. 1980. Influence of biological and physical processes on dissolved oxygen dynamics in an estuarine system: Implications for the measurement of community metabolism. *Estuarine and Coastal Marine Science*, 11(4):407–431.
- Kemp WM, Testa JM. 2012. Metabolic balance between ecosystem production and consumption. In: Wolanski E, McLusky DS, editors, *Treatise on Estuarine and Coastal Science*, pages 83–118. Academic Press, New York.
- Kemp WM, Testa JM, Conley DJ, Gilbert D, Hagy JD. 2009. Temporal responses of coastal hypoxia to nutrient loading and physical controls. *Biogeosciences*, 6(12):2985–3008.
- Murrell MC, Stanley RS, Lehrter JC, Hagy JD. 2013. Plankton community respiration, net ecosystem metabolism, and oxygen dynamics on the Louisiana continental shelf: Implications for hypoxia. *Continental Shelf Research*, 52:27–38.
- Needoba JA, Peterson TD, Johnson KS. 2012. Method for the quantification of aquatic primary production and net ecosystem metabolism using in situ dissolved oxygen sensors. In: Tiquia-Arashiro SM, editor, *Molecular Biological Technologies for Ocean Sensing*, pages 73–101. Springer, New York.
- Nidzieko NJ, Needoba JA, Monismith SG, Johnson KS. 2014. Fortnightly tidal modulations affect net community production in a mesotidal estuary. *Estuaries and Coasts*.
- Nixon SW. 1995. Coastal marine eutrophication: A definition, social causes, and future concerns. *Ophelia*, 41:199–219.
- NRC (National Research Council. 2000. *Clean Coastal Waters: Understanding and Reducing the Effects of Nutrient Pollution*. National Academy Press, Washington, DC.
- Odum HT. 1956. Primary production in flowing waters. *Limnology and Oceanography*, 1(2):102–117.
- Pamatmat MM. 1997. Non-photosynthetic oxygen production and non-respiratory oxygen uptake in the dark: A theory of oxygen dynamics in plankton communities. *Marine Biology*, 129(4):735–746.
- Rabalais NN, Turner RE, Scavia D. 2002. Beyond science into policy: Gulf of Mexico hypoxia and the Mississippi river. *BioScience*, 52(2):129–142.
- RDCT (R Development Core Team). 2014. *R: A language and environment for statistical computing*, v3.1.0. R Foundation for Statistical Computing, Vienna, Austria.
<http://www.R-project.org>.
- Russell MJ, Montagna PA. 2007. Spatial and temporal variability and drivers of net ecosystem metabolism in western Gulf of Mexico estuaries. *Estuaries and Coasts*, 30(1):137–153.
- Sanger DM, Arendt MD, Chen Y, Wenner EL, Holland AF, Edwards D, Caffrey J. 2002. A synthesis of water quality data: National estuarine research reserve system-wide monitoring program (1995-2000). Technical report, National Estuarine Research Reserve Technical Report

595 Series 2002:3. South Carolina Department of Natural Resources, Marine Resources Division
596 Contribution No. 500, Charleston, South Carolina.

597 Short FT, Wyllie-Echeverria S. 1996. Natural and human-induced disturbance of seagrasses.
598 *Environmental Conservation*, 23(1):17–27.

599 Shumway RH, Stoffer DS. 2011. *Time Series Analysis and its Applications: With R Examples*.
600 Springer, New York, New York, 3rd edition.

601 Staehr PA, Bade D, de Bogert MCV, Koch GR, Williamson C, Hanson P, Cole JJ, Kratz T. 2010.
602 Lake metabolism and the diel oxygen technique: State of the science. *Limnology and*
603 *Oceanography: Methods*, 8:628–644.

604 Thébault J, Schraga TS, Cloern JE, Dunlavey EG. 2008. Primary production and carrying
605 capacity of former salt ponds after reconnection to San Francisco Bay. *Wetlands*,
606 28(3):841–851.

607 Tukey JW. 1977. *Exploratory Data Analysis*. Addison-Wesley, Reading, Massachusetts.

608 Wenner E, Sanger D, Arendt M, Holland AF, Chen Y. 2004. Variability in dissolved oxygen and
609 other water-quality variables within the National Estuarine Research Reserve System. *Journal*
610 *of Coastal Research*, 45(SI):17–38.

611 Yin KD, Lin ZF, Ke ZY. 2004. Temporal and spatial distribution of dissolved oxygen in the Pearl
612 River Estuary and adjacent coastal waters. *Continental Shelf Research*, 24(16):1935–1948.

613 Ziegler S, Benner R. 1998. Ecosystem metabolism in a subtropical, seagrass-dominated lagoon.
614 *Marine Ecology Progress Series*, 173:1–12.

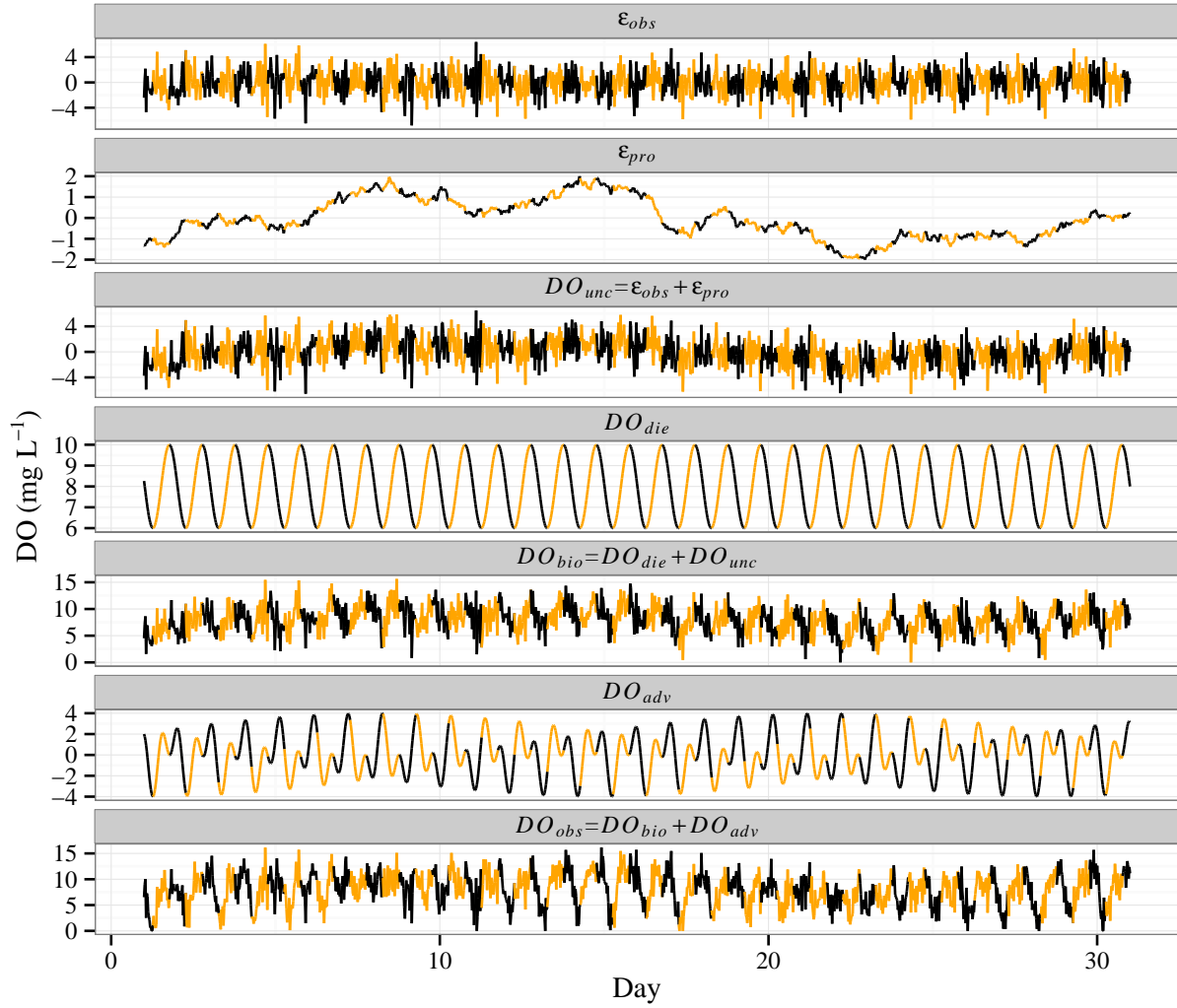


Fig. 1: Example of each component of a simulated DO time series for testing weighted regression. The time series were created using eqs. (4) to (13). Yellow indicates a twelve hour daylight period beginning at 630 each day. fig:do_sim

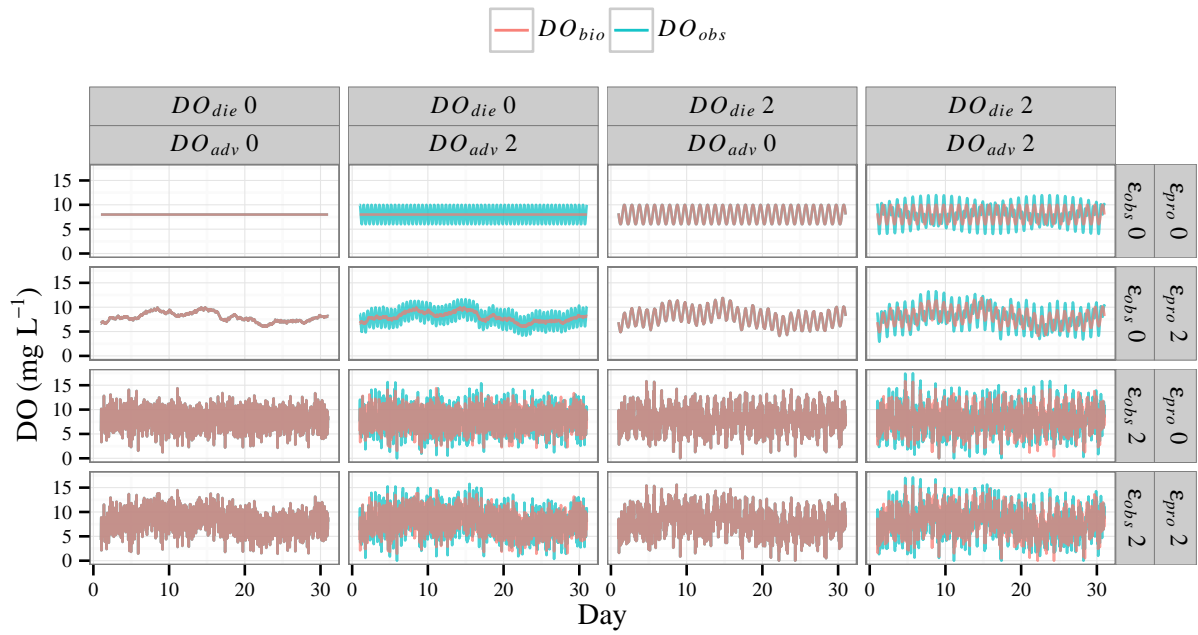


Fig. 2: Representative examples of simulated time series of observed DO (DO_{obs} , blue lines) and biological DO (DO_{bio} , as a component of observed, red lines) created by varying each of four parameters: strength of tidal association with DO signal (DO_{adv}), amount of process uncertainty (ϵ_{pro}), amount of observation uncertainty (ϵ_{obs}), and strength of diel DO component (DO_{die}). Parameter values represent the minimum and maximum used in the simulations as mg L⁻¹ of DO. fig:sim_ex

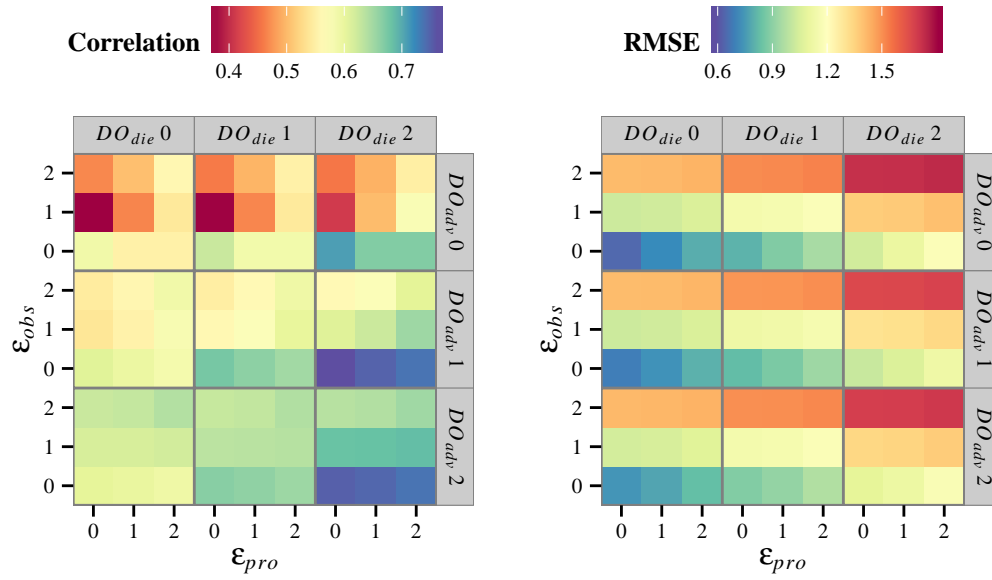


Fig. 3: Heat maps of correlations and errors (RMSE) for filtered DO time series (DO_{dtd}) from weighted regression with ‘true’ biological DO (DO_{bio}) for varying simulation parameters: strength of tidal association with DO signal (DO_{adv}), amount of process uncertainty (ϵ_{pro}), amount of observation observation uncertainty (ϵ_{obs}), and strength of diel DO component (DO_{die}). Each tile represents the correlation or error from results for a given combination of simulation parameters averaged for all window widths (Fig. 4).
fig:err_surfl

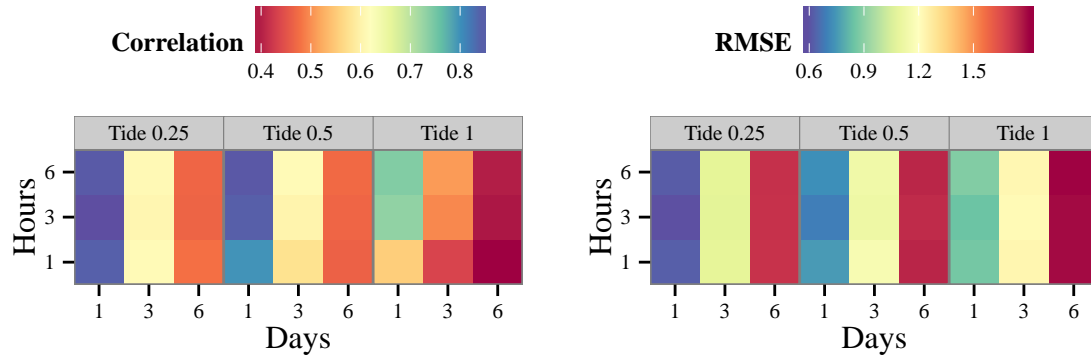


Fig. 4: Heat maps of correlations and errors (RMSE) for filtered DO time series (DO_{dtd}) from weighted regression with ‘true’ biological DO (DO_{bio}) for varying half window widths: days, hour of day, and proportion of tidal range. Each tile represents the correlation or error from results for a given combination of window widths averaged for all simulation parameters (Fig. 3).
fig:err_surf2

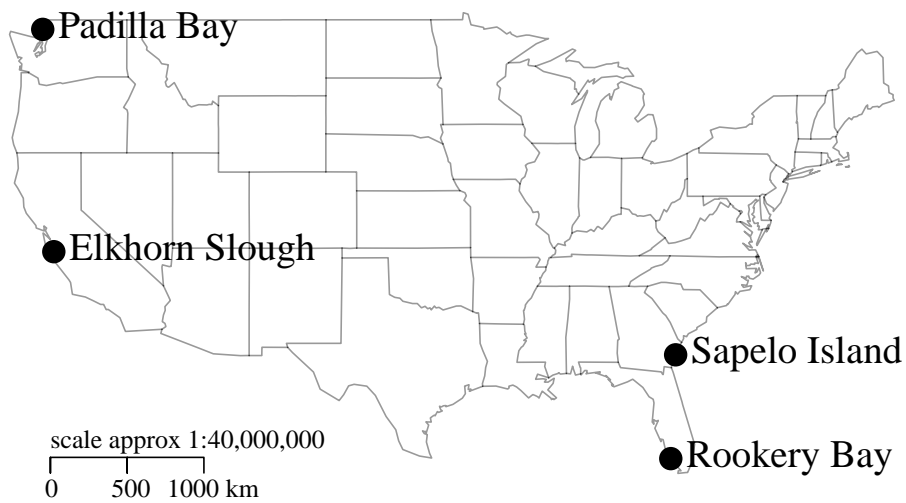


Fig. 5: Locations of NERRS sites used as case studies to validate weighted regression. Stations at each reserve are ELKVM (Vierra Mouth at Elkhorn Slough), PDBBY (Bayview Channel at Padilla Bay), RKBMB (Middle Blackwater River at Rookery Bay), and SAPDC (Dean Creek at Sapelo Island).

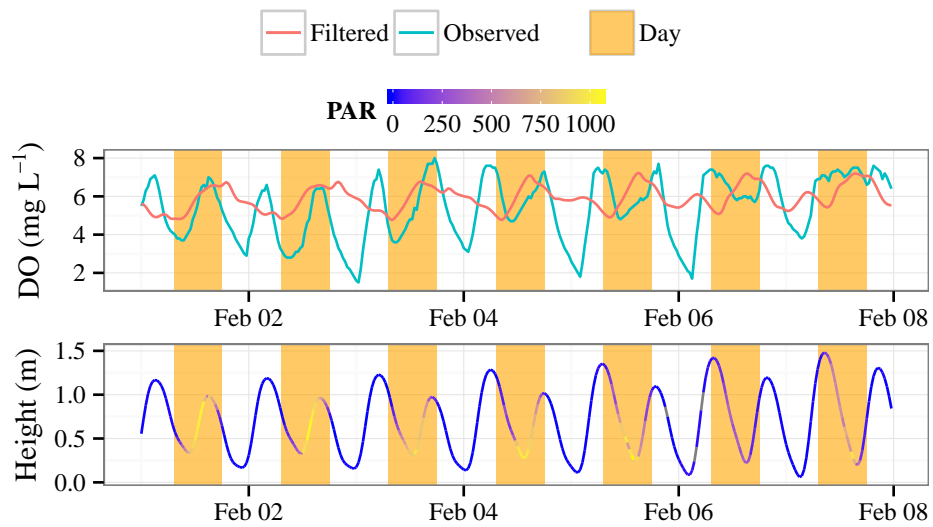


Fig. 6: Continuous DO time series before (observed) and after (filtered) filtering with weighted regression (top) and tidal height (m) colored by total photosynthetically active radiation (bottom, mmol m^{-2}). Results are for the Sapelo Island station for a seven day period when high tide events were out of phase with diel periods, creating lower than expected observed DO during night and day periods. Filtered values are based on a weighted regression with half window widths of six days, one hour within each day, and tidal height proportion of one half.
fig:phase_out

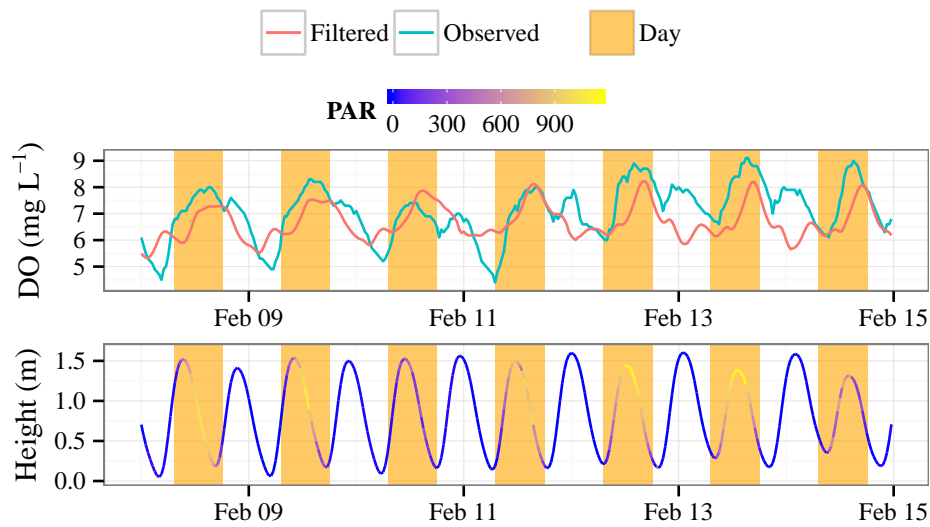


Fig. 7: Continuous DO time series before (observed) and after (filtered) filtering with weighted regression (top) and tidal height (m) colored by total photosynthetically active radiation (bottom, mmol m^{-2}). Results are for the Sapelo Island station for a seven day period when high tide events were in phase with diel periods, creating higher than expected observed DO during night and day periods. Filtered values are based on a weighted regression with half window widths of six days, one hour within each day, and tidal height proportion of one half. ^{fig:phase_in}

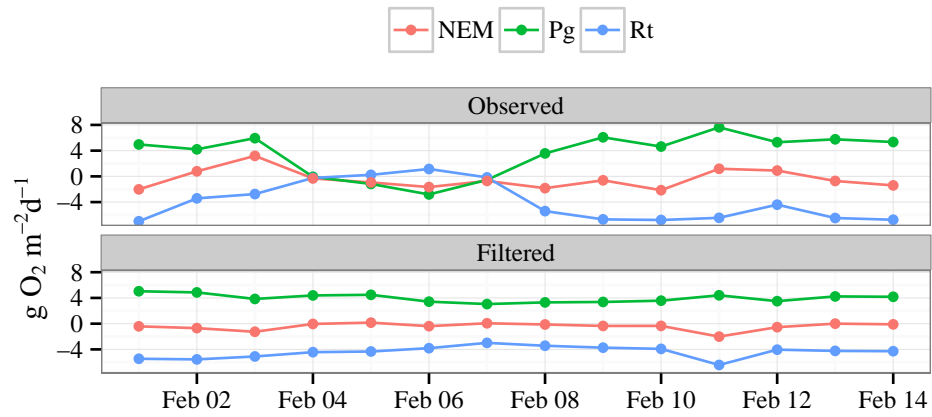


Fig. 8: Example of daily mean metabolism (net ecosystem metabolism, gross production, and total respiration) before (observed) and after (filtered) filtering with weighted regression. Results are for the Sapelo Island station for a two week period in February, 2012 when high tide was out of phase with the diel cycle during the first week (Fig. 6) and in phase during the second week (Fig. 7). fig:case_ex

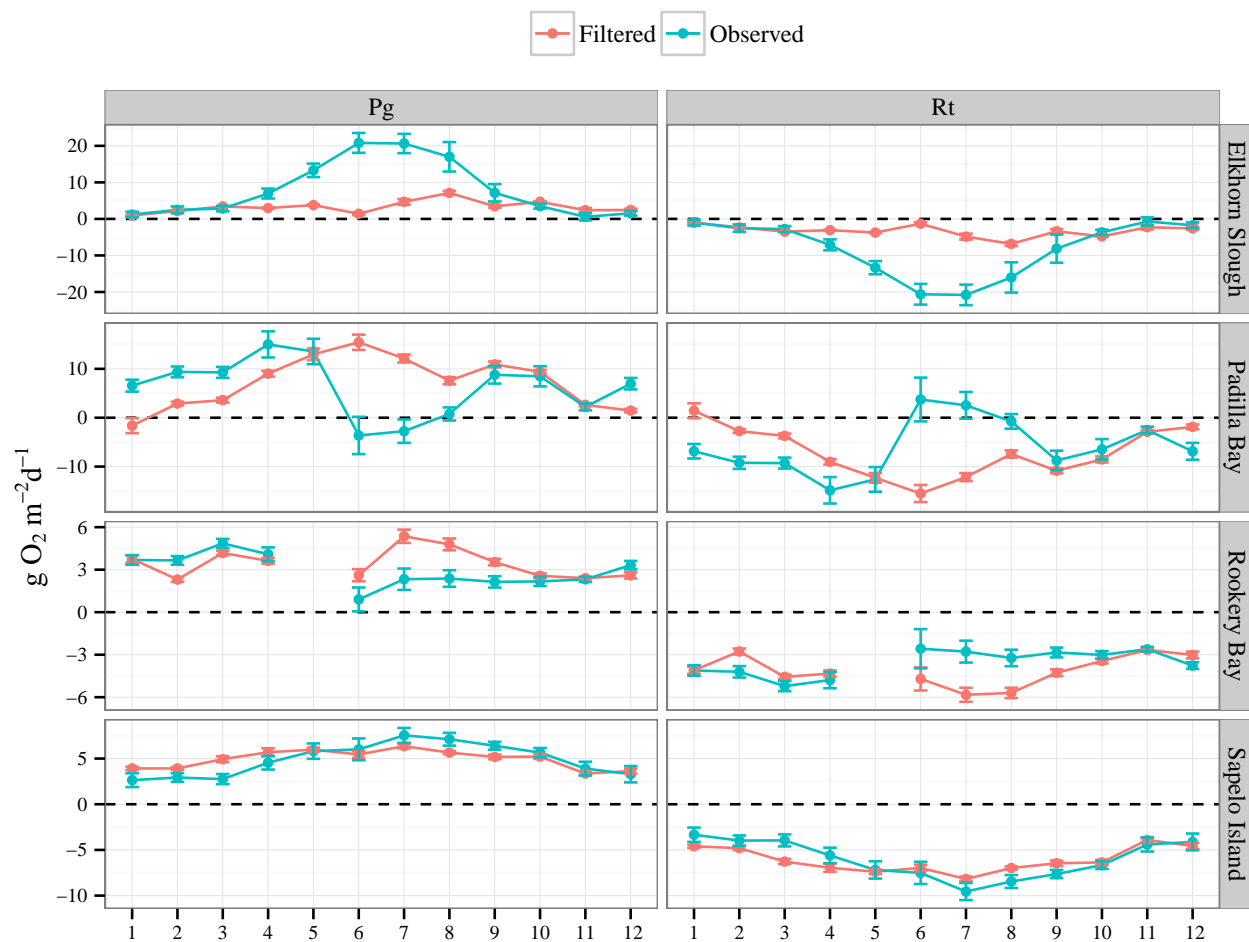


Fig. 9: Means and standard errors of daily metabolism estimates (gross production, total respiration) aggregated by month. Aggregated estimates are shown for observed and filtered DO time series. May was removed from Rookery Bay because of incomplete data.
fig:metab_sum

Table 1: Summary (range, median, quartiles) of correlations and error estimates comparing filtered and biological DO time series for different simulation parameters (DO_{die} , DO_{adv} , ϵ_{pro} , ϵ_{obs}). Values represent averages from multiple simulations with common parameters (e.g., row one is a summary of all simulations for which the diel DO component was zero).
tab:dtd_perfl

Parameter	Correlation					RMSE				
	Min	25 th	Median	75 th	Max	Min	25 th	Median	75 th	Max
DO_{die}										
0	-0.78	0.30	0.51	0.82	1.00	0.00	0.68	1.10	1.97	2.39
1	-0.28	0.38	0.59	0.88	1.00	0.00	0.59	1.07	1.96	2.40
2	-0.39	0.46	0.63	0.90	1.00	0.00	0.62	1.10	1.97	2.40
DO_{adv}										
0	0.00	0.27	0.58	0.93	1.00	0.00	0.34	1.00	1.96	2.12
1	-0.78	0.37	0.58	0.83	1.00	0.00	0.63	1.09	1.98	2.12
2	-0.78	0.47	0.61	0.82	1.00	0.00	0.98	1.34	1.99	2.40
ϵ_{pro}										
0	-0.78	0.34	0.57	0.86	1.00	0.00	0.63	1.06	1.96	2.40
1	-0.78	0.37	0.59	0.85	1.00	0.00	0.63	1.06	1.97	2.40
2	-0.78	0.41	0.61	0.85	1.00	0.00	0.63	1.11	1.98	2.40
ϵ_{obs}										
0	-0.78	0.31	0.82	0.98	1.00	0.00	0.29	0.76	1.50	2.40
1	0.05	0.37	0.58	0.81	0.99	0.07	0.98	1.05	1.49	2.39
2	0.05	0.40	0.58	0.70	0.99	0.15	1.06	1.96	2.01	2.40

Table 2: Summary (range, median, quartiles) of correlations and error estimates comparing filtered and biological DO time series for simulations using different half window widths in the weighted regressions (days, hours, and proportion of tidal range). Values represent averages from multiple simulations with common window values (e.g., row one is a summary of all simulations for which the half window width was one day).^{tab:dtd_perf2}

Window	Correlation					RMSE				
	Min	25 th	Median	75 th	Max	Min	25 th	Median	75 th	Max
Days										
1	-0.78	0.63	0.89	0.97	1.00	0.00	0.28	0.59	1.04	2.12
3	-0.07	0.40	0.59	0.75	1.00	0.00	0.99	1.08	1.28	2.08
6	0.00	0.26	0.40	0.58	1.00	0.00	1.95	1.98	2.05	2.40
Hours										
1	-0.78	0.36	0.58	0.82	1.00	0.00	0.63	1.11	1.96	2.40
3	0.00	0.40	0.60	0.87	1.00	0.00	0.58	1.07	1.97	2.36
6	0.03	0.37	0.59	0.85	1.00	0.00	0.64	1.10	1.98	2.40
Tide										
0.25	0.00	0.42	0.63	0.91	1.00	0.00	0.51	1.04	1.97	2.21
0.5	0.06	0.43	0.62	0.88	1.00	0.00	0.61	1.09	1.97	2.27
1	-0.78	0.30	0.51	0.79	1.00	0.00	0.73	1.20	1.97	2.40

Table 3: Summary statistics of tidal component amplitudes (m), selected water quality parameters (DO mg L⁻¹, chlorophyll-a μ g L⁻¹, salinity psu, water temperature °C) and metabolism estimates (gross production, respiration, and net ecosystem metabolism as g m⁻² d⁻¹) for each case study. Tidal components are principal lunar semidiurnal (O1, frequency 25.82 hours), solar diurnal (P1, 24.07 hours), lunar semidiurnal (M2, 12.42 hours), and solar semidiurnal (S2, 12 hours) estimated from harmonic regressions of tidal height (oce package in R, [Foreman and Henry 1989](#), [RDCT 2014](#)). Water quality data are averages for the entire period of record for each site. Metabolism estimates are means of daily integrated values.^{tab:case_att}

Site	Tidal amplitude				Water quality				Metabolism ^a		
	O1	P1	M2	S2	DO	Chl	Sal	Temp	Pg	Rt	NEM
ELKVM	0.24	0.12	0.48	0.13	7.87	3.87	32.43	13.78	8.14	-8.19	-0.05
PDBBY	0.46	0.23	0.63	0.15	8.97	2.24	29.17	10.44	5.95	-5.90	0.05
RKBMB	0.13	0.04	0.36	0.10	4.48	4.50	30.53	25.85	3.02	-3.62	-0.60
SAPDC	0.10	0.02	0.54	0.07	4.96	5.98	27.30	21.77	4.89	-6.04	-1.16

^aPg: gross production, Rt: respiration, NEM: net ecosystem metabolism

Table 4: Correlations of tidal changes at each site with continuous DO observations and metabolism estimates (gross production, respiration, and net metabolism) before (observed) and after (filtered) filtering with weighted regression. Values are averages of monthly correlations. DO values are correlated with predicted tidal height at each observation, whereas metabolism estimates are correlated with mean tidal height change between observations during day, night, or total day periods for production, respiration, and net metabolism, respectively.

Site	DO	Pg ^a	Rt	NEM
ELKVM				
Observed	0.44	0.43	0.43	0.33
Filtered	-0.04	0.04	-0.01	0.09
PDBBY				
Observed	-0.49	-0.11	-0.29	-0.28
Filtered	0.01	-0.05	0.00	-0.33
RKBMB				
Observed	0.45	0.26	0.34	0.30
Filtered	0.02	-0.04	0.03	0.10
SAPDC				
Observed	0.62	0.47	0.64	0.43
Filtered	0.00	-0.04	0.07	-0.04

^aPg: gross production, Rt: respiration, NEM: net ecosystem metabolism

Table 5: Summary of metabolism estimates (gross production, respiration, and net metabolism) for case studies using DO time series before (observed) and after (filtered) filtering with weighted regression. Means and standard errors are based on daily integrated metabolism estimates. Anomalous values are the proportion of metabolism estimates that were negative for gross production and positive for respiration. Results are for weighted regressions with half window widths of six days, one hour within each day, and a tidal height proportion of one half.^{tab:case_res}

Site	Pg^a			Rt			NEM	
	Mean	Std. Err.	Anom	Mean	Std. Err.	Anom	Mean	Std. Err.
ELKVM								
Observed	8.14	0.67	0.19	-8.19	0.69	0.21	-0.05	0.16
Filtered	3.00	0.13	0.07	-3.06	0.14	0.07	-0.06	0.02
PDBBY								
Observed	5.95	0.69	0.22	-5.90	0.74	0.19	0.05	0.22
Filtered	7.01	0.40	0.05	-7.01	0.40	0.06	0.00	0.07
RKBMB								
Observed	3.02	0.14	0.09	-3.62	0.15	0.08	-0.60	0.06
Filtered	3.46	0.10	0.01	-4.07	0.11	0.01	-0.61	0.04
SAPDC								
Observed	4.89	0.23	0.13	-6.04	0.25	0.11	-1.16	0.09
Filtered	4.94	0.09	0.00	-6.13	0.10	0.00	-1.19	0.05

^aPg: gross production, Rt: respiration, NEM: net ecosystem metabolism

Multimedia

{multi}

The supporting information for this manuscript includes a graphical illustration of the weighting scheme described in the material and procedures section (http://spark.rstudio.com/beckmw/weights_widget), results for each simulation (http://spark.rstudio.com/beckmw/detiding_sims), and results for each case study (http://spark.rstudio.com/beckmw/detiding_cases). Each link is a graphical summary of data based on interactive inputs to support the results in the manuscript.